8

Intracellular signalling during bacterial chemotaxis

Marcus J. Tindall, Philip K. Maini, Judy P. Armitage, Colin Singleton and Amy Mason

1 Bacterial chemotaxis

Chemotactic bacteria are some of the best studied systems in biology. Their behaviour on the single cell and population scale has been investigated for the past 30 plus years both by experimentalists and theoreticians. Indeed work undertaken in this area is a paradigm of the success of mathematical modelling in helping to understand biological systems, even before the advent of 'systems biology'. However, although we know much of the biochemistry and basic characteristics of the systems, there remain a number of unanswered questions, both on the individual and collective population scale, about chemotactic bacteria.

Bacteria such as *E. coli* and *R. sphaeroides* respond to changes in extracellular attractant levels by changing the pattern of rotation of their flagella anchored across the cell membrane (Eisenbach *et al.*, 2004). In the case of *E. coli* changes in attractant concentration are detected by membrane-spanning methyl-accepting chemotaxis proteins (MCPs) at the poles of the rod-like shaped bacteria. Through a number of intracellular phosphotransfer biochemical reactions, these changes are communicated to the FliM protein motors that switch the direction of flagellar rotation. In the case of *E. coli*, the default setting of clockwise rotations in the absence of an attractant gradient, interspersed with periodic switching to clockwise rotation, leads to a series of run and tumbles. During such movement the individual four to six flagella rotate together to form a bundle which leads to short bursts of directed motion, followed by tumbling as a result of one or more flagella switching. Tumbling re-orientates the bacterium on a different directional heading each time. Considered over the order of minutes this movement leads to three-dimensional random-walk-like behaviour. When a change in the external concentration level of an attractant is detected by the MCPs, the bacterial flagella rotate for longer in a counter-clockwise direction leading to extended periods of runs up the attractant gradient resulting in chemotaxis.

If so much is known about bacterial chemotactic species, in particular *E. coli*, why do we continue to study them? The answer lies in the intriguing behaviour and characteristics these systems exhibit. For instance, *E. coli* are able to sense and respond to only small changes in attractant concentration (experimentally observed as small as the order of a few molecules; Segall *et al.*, 1986). This ability to magnify the effect of

attractant binding in order to initiate the biochemical cascade between the receptors and the motors has been observed to be as high as 35 times the initial binding intensity (Sourjik and Berg, 2002b). Such a magnification is commonly referred to as gain and the mechanism for obtaining it has been of great interest to researchers for a number of years. Bacteria are also able to detect changes in concentration levels across five orders of magnitude, responding robustly in each case. Given the availability of data, both on the individual and population scale, mathematical models can be utilized to assist in explaining such observed characteristics.

Mathematical modelling has been particularly influential in the field of bacterial chemotaxis. A wide range of mathematical approaches have been used to help understand particular aspects of bacterial chemotactic systems, both on the individual and population scale (Tindall *et al.*, in press). Modelling work has often been undertaken in conjunction with experiment as we detail in Section 3. Mathematical models have been developed to explain experimental observations, verified against such observations and used to generate new hypotheses which are then experimentally tested. In other cases purely hypothetically based models have been formulated to explain biologically observed phenomena, for instance in the case of receptor–receptor interactions (Bray *et al.*, 1998).

In the work to be presented and discussed here we will focus specifically on the role of intracellular signalling within *E. coli*. A mathematical model will be developed to predict how the concentration of certain intracellular proteins affects the overall receptor-to-motor response of a bacterium. Importantly our modelling technique differs from previous models in that it seeks to simultaneously account for the effects that both spatial localization of the proteins and their predefined interactions have on the overall behaviour of the network. Generally, work in this area has focused primarily on modelling only the temporal dynamics, ignoring spatial aspects of the problem (Tindall *et al.*, in press). Our modelling technique will be compared with others to demonstrate both its usefulness and shortcomings.

Before presenting our specific modelling example we detail the known biological facts of the intracellular signalling pathway within *E. coli* in Section 2. Section 3 provides a brief overview of mathematical modelling in understanding various aspects of bacterial chemotaxis systems. In Section 4 we present a spatio-temporal mathematical model of the phosphotransfer pathway within *E. coli* specifically focusing on the proteins responsible for signalling between the membrane receptors and flagellar motors. Results from the model are presented and the effects of the outcomes discussed. The results of our work and the application of mathematical modelling in this and other fields of systems biology are discussed in Section 5.

2 Intracellular signalling within bacterial chemotaxis

Generally bacteria are too small in length (around 1–3 μm) to be able to detect spatial changes in their external attractant concentration. Instead they rely on an internal temporal system of biochemical signalling to communicate changes in the external environment via their MCPs to the flagella motors (Wadhams and Armitage, 2004). This internal intracellular network can range in complexity amongst various species of bacteria (Porter *et al.*, 2006; Rao *et al.*, 2004). In the case of *E. coli*, the internal phosphotransfer reaction is mediated by the activation of proteins associated with the

MCPs, primarily chemotaxis protein A (CheA) and CheW. CheW is thought to bind CheA to the cytoplasmic domain of the MCP receptor. In the absence of an attractant gradient, CheA autophosphorylates. The resulting phosphoryl groups are then transferred from the phosphorylated CheA protein molecules ($CheA_P$) to two proteins: CheB and CheY. CheY is an abundant protein within the bacterial cytoplasm. Diffusing from the receptors through the cytoplasm, phosphorylated CheY ($CheY_P$) is then free to interact with FliM protein motors which regulate the flagella switching. This interaction leads to the clockwise rotation of the flagella causing random walk behaviour. The protein CheZ actively dephosphorylates $CheY_P$ ($CheY_P$ also dephosphorylates naturally on a slower timescale).

The phosphoryl transfer from $CheA_P$ to CheB activates the esterase activity of CheB which demethylates the MCPs. This action of demethylation dynamically counteracts constant methylation of the receptors by the transferase protein CheR. Receptor methylation plays an important role in bacterial chemotaxis – it allows the system time to adapt to changes in different concentrations of the extracellular nutrient concentration. Whilst the initial change in motor bias is rapid (of the order of 100s of milliseconds), adaptation of the bacterium is relatively slow (of the order of up to 60 seconds). This period of delayed adaptation allows the bacterium time to undertake periods of extended runs and also attenuate its ability to detect new changes in the attractant concentration. It is through a careful balance of methylation of the receptors, which reduces sensitivity to bound attractant molecules, and demethylation, which increases sensitivity, that adaptation is achieved.

On detecting an increase in attractant concentration, through binding of attractant molecules to the receptors, the autophosphorylation of CheA is inhibited, thus leading to a drop in $CheY_P$ levels and subsequent counter-clockwise rotation of the flagella motors. Likewise $CheB_P$ levels fall and methylation of the receptors follows as a result of the constant activity of CheR. The increased methylation of the receptors finally leads to reactivation of the autophosphorylation of CheA, thereby resetting the system to its pre-stimulus levels. The details of the phosphotransfer process are summarized in *Figure 1* and each reaction is listed in *Table 1*.

3 Mathematical modelling and bacterial chemotaxis

Mathematical modelling is a useful and powerful tool for understanding and elucidating aspects of physical and biological systems. In order to build useful and informative models, certain aspects of the system must already be understood. A model can then be formulated and the respective model outcomes used to predict the behaviour of the system. Model outcomes are initially tested against known experimental results in order to verify the model. Certain attributes of the model (describing physical characteristics of the system) can then be altered to understand how they affect the outcomes, thus making predictions about the system's behaviour. Models can therefore be used to test experimental hypotheses and also direct future experimental work.

We note here that applied mathematical modelling does not constitute statistics or related fields such as bioinformatics, but instead focuses on understanding the 'system' by explaining its observed characteristics. Many aspects of such modelling are inherent in what is now commonly termed systems biology.

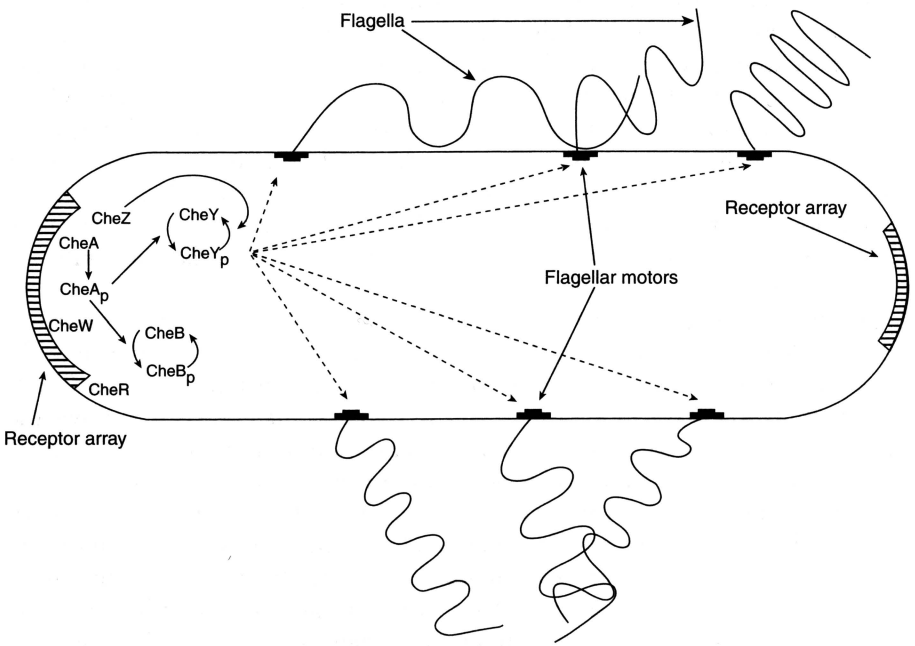

Figure 1. *A schematic representation (not to scale) of a typical* E. coli *bacterium (approximately 3 μm long) showing the location of the membrane receptors and flagella. CheW binds CheA to the cytoplasmic receptor domains. A decrease of attractant causes CheA to autophosphorylate, the phosphorylated CheA, $CheA_P$, passes the phosphoryl groups to both CheY and CheB. The subsequently phosphorylated CheY diffuses (indicated schematically by the dotted lines) to the flagellar motors where it causes them to rotate in a clockwise direction. $CheY_P$ can be dephosphorylated by CheZ. The phosphotransfer to CheB ensures that it acts to negate the methylating action of CheR, thus reducing the receptor methylation state. With the addition of attractant, the rate of autophosphorylation of CheA is reduced and thus $CheY_P$ levels fall. The motors respond to the drop in $CheY_P$ by rotating counter-clockwise causing the flagella to bundle together leading to runs. The dephosphorylation of $CheB_P$ allows CheR to further methylate the receptors thus inducing further $CheA_P$ activity, thereby returning the system to its pre-stimulus configuration.*

Many elements of the bacterial chemotaxis system, both on the individual and population scale, have been the subject of mathematical models for more than 40 years. The original application of mathematical modelling was used to understand the experimental assay work of Adler (Adler, 1966), who observed the migration of *E. coli* up gradients of attractant within a capillary tube (Keller and Segel, 1971). The modelling work focused on various different forms of the bacterial diffusion and chemotactic coefficients, thus seeking, in a somewhat coarse-grain fashion, to understand how microscale individual behaviour affected the macroscale population behaviour (Tindall *et al.*, in press).

Modelling of individual bacteria was motivated around the same time as the work of Adler by the work of Berg and colleagues (Block *et al.*, 1982, 1983), who observed

Table 1. *The autophosphorylation, phosphotransfer and dephosphorylation reactions within* E. coli.

Process	Reaction	Details
Autophosphorylation	$CheA \xrightarrow{k_1} CheA_P$	
Phosphotransfer	$CheA_P + CheY \xrightarrow{k_2} CheA + CheY_P$	$CheA_P$ to CheY
	$CheA_P + CheB \xrightarrow{k_3} CheA + CheB_P$	$CheA_P$ to CheB
Dephosphorylation	$CheY_P + CheZ \xrightarrow{k_4} CheY + CheZ$	Dephosphorylation by CheZ
	$CheB_P \xrightarrow{k_5} CheB$	Natural dephosphorylation
	$CheY_P \xrightarrow{k_6} CheY$	Natural dephosphorylation

the attractant response behaviour of individual bacteria. Their subsequent findings on the interesting excitation and adaptation response of bacteria, and later work by Segall *et al.* (1986) on the highly sensitive response of the system to only small changes in the attractant concentration, has seen mathematical models used to understand particular elements of the bacterial system. Adaptation, sensitivity, gain or flagella dynamics, through to looking at the particular physical aspects of the bacterium, for example receptor dynamics, the phosphotransfer pathway, protein–motor interactions, and so on, have all been fertile areas. The growth in modelling sophistication has occurred in parallel with the ever-increasing understanding of the underlying biology. For instance, in the case of adaptation, early efforts focused on describing a number of basic receptor state models which relied on receptors being either attractant-bound or unbound, in either case moving between an inactive or active state (Goldbeter and Koshland, 1982; Segel and Goldbeter, 1986). Such inactive or active states were precursors to the discovery of the role of methylation in changing receptor activity, and later the proteins responsible for affecting this (CheR and $CheB_P$). With increasing understanding of the phosphotransfer pathway in the late 1980s and throughout the 1990s, the phosphotransfer pathway and role of CheR and $CheB_P$ in affecting methylation have been introduced to more recent models on adaptation and sensitivity (Barkai and Leibler, 1997; Spiro *et al.*, 1997).

The role of modelling has been particularly helpful in elucidating possible mechanisms responsible for sensitivity. With the advent of modelling of the phosphotransfer pathway within *E. coli* it was evident that a model of the pathway alone could not provide the necessary sensitivity and gain observed experimentally (Bray *et al.*, 1993; Spiro *et al.*, 1997). In using a discrete model in which receptors interact with one another to magnify the initial response of only one activated receptor through attractant binding, Bray and colleagues (Bray *et al.*, 1998) were able to show that this was a plausible mechanism for explaining both sensitivity and gain. Subsequent research, both experimental and theoretical, has focused on establishing the exact biochemical and physical forms of these interactions.

More recently, models of transport events within bacteria have focused on the role that the spatial environment within bacteria plays in affecting the phosphotransfer interaction between the receptors and flagellar motors (Lipkow *et al.*, 2005; Lipkow, 2006). Here the effect of CheZ localization on the distribution of $CheY_P$ throughout the cytoplasm of the cell has been considered. Lipkow *et al.* (2005) found that when CheZ was allowed to diffuse throughout the cell, the $CheY_P$ concentration decreased exponentially from the receptor poles to the motors. However, when CheZ was localized to the membrane receptor regions of a cell, the concentration of $CheY_P$ was approximately constant throughout the cell, a result which agreed with experimental findings (Cantwell *et al.*, 2003; Liberman *et al.*, 2004).

With the growth of computing power and the sophistication of models both on the individual and population scale, the modelling of bacterial chemotaxis systems is heading towards more sophisticated multi-scale modelling techniques – where models on the individual scale are computed for a given population of cells (Bray *et al.*, 2007, Emonet *et al.*, 2005; Erban and Othmer, 2004; Kreft *et al.*, 1998). The motivation for such work is to understand how individual cell behaviour affects the overall collective behaviour of the population. Such work has clear benefits, for example, in helping to understand biofilm behaviour, a consistent problem in medicine and the industrial world.

The more sophisticated a model on the individual cell level is, the more time it takes to integrate the respective input and provide output, thus when this is multiplied by the number of cells typical of a population the computational power required to provide answers in a feasible period of time will be very large. We are therefore faced with a 'double-edged' sword in that models must provide the relevant characteristics observed on the individual scale, but not become so sophisticated that understanding behaviour on the population scale becomes infeasible – so called 'model reduction'. Such work continues to provide challenges for mathematical modellers and experimentalists in seeking to understand bacterial chemotactic systems.

4 Developing a model of intracellular signalling

The focus of our work here is to understand how the spatio-temporal concentration of $CheY_P$ within a cell is dynamically affected by the removal of attractant from the bacterial receptors. What is the most appropriate mathematical modelling method for tackling this problem? It is worth noting that given the richness of mathematical theory and modelling approaches there are a number of choices. Should we consider modelling each individual protein molecule and its kinetics? How are we to include both the spatial and reaction processes simultaneously? Are stochastic effects important? Will our model be computationally efficient, that is, can it be solved in a reasonable period of time? How do we verify our model?

In order to develop an appropriate mathematical model we note that: (i) our theory needs to describe both the spatial localization of the respective proteins in time and a defined spatial region; and (ii) reaction rates and diffusion coefficients of the respective proteins are known from *in vitro* data (see *Table 2*). Given the reactions are known and the copy number (concentration) of each protein within the cytoplasm is high (see http://www.pdn.cam.ac.uk/groups/comp-cell/Rates.html for details), we can adopt an averaging approach in modelling individual protein molecules (both in space and time).

Table 2. *Dimensional and non-dimensional parameter values.*

Rate	Description	Value	Reference
k_1	Autophosphorylation of CheA	34 s^{-1}	Francis *et al.* (2002) Shrout *et al.* (2003)
k_2	Phosphotransfer from $CheA_P$ to CheY	1×10^8 $(Ms)^{-1}$	Stewart *et al.* (2000)
k_4	$CheY_P$ dephosphorylation by CheZ	1.6×10^6 $(Ms)^{-1}$	Li and Hazelbauer (2004) Sourjik and Berg (2002a)
k_6	$CheY_P$ natural dephosphorylation	8.5×10^{-2} s^{-1}	Smith *et al.* (2003) Stewart and van Bruggen (2004)
D_{Y_p}	$CheY_P$ diffusion coefficient	10 μm^2 s^{-1}	Elowitz *et al.* (1999) Segall *et al.* (1985)
A_T	Total CheA concentration in an *E. coli* cell	7.9 μm	Bray website data[1]
Y_T	Total CheY concentration in an *E. coli* cell	9.7 μm	Bray website data
Z	Total CheZ concentration in an *E. coli* cell	3.8 μm	Bray website data
$\bar{k}_2$	Non-dimensional phosphotransfer from CheAp to CheY.	28.53	–
$\bar{k}_4$	Non-dimensional CheYp dephosphorylation by CheZ.	0.179	–
$\bar{k}_6$	Non-dimensional CheYp natural dephosphorylation	2.5×10^{-3}	–
α	Ratio of total CheA to CheY concentration	0.814	–
$\bar{D}_Y$	Non-dimensional diffusion coefficient	1	–

[1] www.pdn.cam.ac.uk/groups/comp-cell/Rates.html

These points lead us to adopt the continuum mathematical theory of reaction-diffusion equations (Murray, 1993). Our system of governing partial differential equations (PDEs) will be of the form:

$$\frac{\partial v}{\partial t} = D_u \nabla^2 u + f(u,v), \tag{1}$$

$$\frac{\partial v}{\partial t} = D_v \nabla^2 u + g(u,v). \tag{2}$$

Here $u = u(\mathbf{x},t)$ and $v = v(\mathbf{x},t)$ are the concentrations of two proteins at spatial points $\mathbf{x} = (x,y,z)$ and time t, where the functions $f(u,v)$ and $g(u,v)$ describe the reactions between each protein. We have assumed the diffusion coefficients D_u and D_v are constant and isotropic and in the case of three-dimensional geometry

$$\nabla^2 = \frac{\partial^2}{\partial x^2} + \frac{\partial^2}{\partial y^2} + \frac{\partial^2}{\partial z^2}.$$

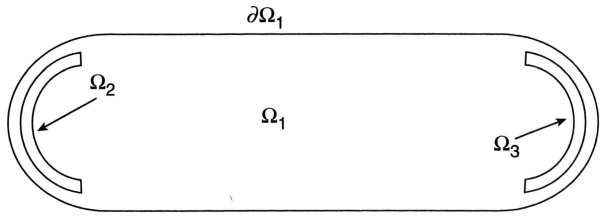

Figure 2. *A schematic representation of our two-dimensional model of an* E. coli *cell.* Ω_2 *and* Ω_3 *represent the regions near the receptor clusters in which CheA and* $CheA_P$ *are generally found. The outer boundary of the cell is denoted by* $\partial\Omega_1$ *and the remaining cytoplasmic region by* Ω_1.

This term (along with the diffusion coefficient) represents diffusion of the respective protein within the defined region of interest.

Given the symmetry of a cell along its length we only need to consider two-dimensional slices of the cytoplasmic region. Such a model can be solved computationally in a realistic time and in some cases, analytical approximations of the way in which the protein concentrations vary as a function of parameters within the model can be found.

Our system of equations is solved on the model cell shown in *Figure 2* based upon the following assumptions. We consider only phosphotransfer between $CheA_P$ and $CheY_P$ and the effect of CheZ. We neglect phosphotransfer to CheB given that it is concerned with local methylation of the receptors and not receptor-to-motor signalling. The role of $CheB_P$ will be included in future work as discussed in Section 5. We further assume that CheA, $CheA_P$ and CheZ are restricted to the two regions Ω_2 and Ω_3. CheA and $CheA_P$ are immobile in each region and the concentration of CheZ remains constant for all time. These regions are designed to represent the localization of CheA and $CheA_P$ to receptor clusters within the cell membrane. CheY and $CheY_P$ are free to diffuse throughout the full cytoplasmic region $(\Omega_1 \cup \Omega_2 \cup \Omega_3)$.

Invoking the law of mass-action (Murray, 1993) we can write down a set of reaction-diffusion equations governing each of the relevant reactions detailed in *Table 1* (neglecting CheB).

In the regions Ω_2 and Ω_3:

$$\frac{\partial A}{\partial t} = -k_1 A + k_2 A_p Y, \tag{3}$$

$$\frac{\partial A_p}{\partial t} = k_1 A - k_2 A_p Y, \tag{4}$$

$$\frac{\partial Y}{\partial t} = D_Y \nabla^2 Y - k_2 A_p Y + k_4 Y_p Z + k_6 Y_p, \tag{5}$$

$$\frac{\partial Y_p}{\partial t} = D_{Y_p} \nabla^2 Y_p + k_2 A_p Y - k_4 Y_p Z - k_6 Y_p, \tag{6}$$

and in Ω_1

$$\frac{\partial Y}{\partial t} = D_Y \nabla^2 Y + k_6 Y_P, \tag{7}$$

$$\frac{\partial Y_P}{\partial t} = D_{Y_P} \nabla^2 Y_P - k_6 Y_P. \tag{8}$$

Here A = [CheA], A_P = [CheA$_P$], Y = [CheY], Y_P = [CheY$_P$] and Z = [CheZ] and the respective reaction rates and diffusion coefficients are detailed in *Table 2*. The initial distribution of CheA (see below) fills both Ω_2 and Ω_3, and neither CheA nor CheA$_P$ are assumed to diffuse within the respective regions (one is simply converted to the other and vice-versa) or outside them. CheZ is also assumed to remain constant within this region and thus we do not require an equation describing any changes in its concentration, either spatially or dynamically. The diffusion coefficients for CheY and CheY$_P$ are assumed to be the same in each of the three regions. We note here that given we are only considering a two-dimensional region:

$$\nabla^2 = \frac{\partial^2}{\partial x^2} + \frac{\partial^2}{\partial y^2}.$$

In order to complete or close our system of equations we need to define a set of initial and boundary conditions. Initial conditions define the initial protein concentration at time $t = 0$ in each region and boundary conditions detail the concentration on the boundary of the region (denoted as $\partial\Omega_1$ in *Figure 2*) for all time.

We assume initially that only CheA is present in each of the receptor regions Ω_2 and Ω_3 and CheZ is constant throughout these regions. All other protein concentrations are zero. These conditions can be defined mathematically as follows.

In ω_1 we have

$$Y(\mathbf{x},0) = Y_0 \qquad \text{and} \qquad Y_P(\mathbf{x},0) = 0 \tag{9}$$

and in Ω_2 and Ω_3

$$A(\mathbf{x},0) = A_0,\ A_P(\mathbf{x},0) = 0,\ Y(\mathbf{x},0) = Y_0 \text{ and } Y_P(\mathbf{x},0) = 0. \tag{10}$$

Here A_0 is the initial concentration of CheA, Y_0 the initial concentration of CheY. For computational reasons an appropriately smooth function is chosen to represent A_0.

We assume no flux boundary conditions on $\partial\Omega_1$ which equates to neither CheY nor CheY$_P$ being able to diffuse outside the cell wall boundary

$$\hat{\mathbf{n}} \cdot \nabla Y(\mathbf{x},t) = 0 \text{ and } \hat{\mathbf{n}} \cdot \nabla Y_P(\mathbf{x},t) = 0. \tag{11}$$

Here $\hat{\mathbf{n}}$ is a unit vector normal to the surface of the cell. The flux of CheY and CheY$_P$ is taken to be continuous between each of the three regions Ω_1, Ω_2 and Ω_3.

$$\frac{\partial Y}{\partial t} = D_Y \nabla^2 Y + k_6 Y_P, \tag{7}$$

$$\frac{\partial Y_P}{\partial t} = D_{Y_P} \nabla^2 Y_P - k_6 Y_P. \tag{8}$$

Here A = [CheA], A_P = [CheA$_P$], Y = [CheY], Y_P = [CheY$_P$] and Z = [CheZ] and the respective reaction rates and diffusion coefficients are detailed in *Table 2*. The initial distribution of CheA (see below) fills both Ω_2 and Ω_3, and neither CheA nor CheA$_P$ are assumed to diffuse within the respective regions (one is simply converted to the other and vice-versa) or outside them. CheZ is also assumed to remain constant within this region and thus we do not require an equation describing any changes in its concentration, either spatially or dynamically. The diffusion coefficients for CheY and CheY$_P$ are assumed to be the same in each of the three regions. We note here that given we are only considering a two-dimensional region:

$$\nabla^2 = \frac{\partial^2}{\partial x^2} + \frac{\partial^2}{\partial y^2}.$$

In order to complete or close our system of equations we need to define a set of initial and boundary conditions. Initial conditions define the initial protein concentration at time $t = 0$ in each region and boundary conditions detail the concentration on the boundary of the region (denoted as $\partial\Omega_1$ in *Figure 2*) for all time.

We assume initially that only CheA is present in each of the receptor regions Ω_2 and Ω_3 and CheZ is constant throughout these regions. All other protein concentrations are zero. These conditions can be defined mathematically as follows.

In ω_1 we have

$$Y(\mathbf{x},0) = Y_0 \qquad \text{and} \qquad Y_P(\mathbf{x},0) = 0 \tag{9}$$

and in Ω_2 and Ω_3

$$A(\mathbf{x},0) = A_0,\ A_P(\mathbf{x},0) = 0,\ Y(\mathbf{x},0) = Y_0 \text{ and } Y_P(\mathbf{x},0) = 0. \tag{10}$$

Here A_0 is the initial concentration of CheA, Y_0 the initial concentration of CheY. For computational reasons an appropriately smooth function is chosen to represent A_0.

We assume no flux boundary conditions on $\partial\Omega_1$ which equates to neither CheY nor CheY$_P$ being able to diffuse outside the cell wall boundary

$$\hat{\mathbf{n}} \cdot \nabla Y(\mathbf{x},t) = 0 \text{ and } \hat{\mathbf{n}} \cdot \nabla Y_P(\mathbf{x},t) = 0. \tag{11}$$

Here $\hat{\mathbf{n}}$ is a unit vector normal to the surface of the cell. The flux of CheY and CheY$_P$ is taken to be continuous between each of the three regions Ω_1, Ω_2 and Ω_3.

4.1 Non-dimensionalization

Before attempting to solve the model, the dimensions from the governing equations are removed. Why do we do this? Non-dimensionalization refers to removing the dimensions from our equations. This allows consideration to be given to the effect that certain terms in our equations have in comparison to others. The relative magnitude of each can then be more clearly judged. Furthermore it reduces the number of parameters in our model.

Our governing equations contain both a lengthscale and a timescale and the governing equations are rescaled with respect to these. Here we non-dimensionalize with respect to the timescale of autophosphorylation of CheA (k_1) and the length scale associated with the diffusion distance of $CheY_P$ through the cell

$$t = \frac{\tau}{k_1} \quad \text{and} \quad \mathbf{x} = \sqrt{\frac{D_{Y_P}}{k_1}}\hat{\mathbf{x}}. \tag{12}$$

Here τ and $\hat{\mathbf{x}}$ are the non-dimensional timescales and length scales, respectively. The concentration of CheA, $CheA_P$, CheY and $CheY_P$ are rescaled with respect to the total phosphorylated and unphosphorylated CheA and CheY concentrations within the cell, A_T and Y_T, respectively

$$A = A_T\hat{A}, \qquad A_P = A_T\hat{A}_P, \qquad Y = Y_T\hat{Y} \text{ and } \qquad Y_P = Y_T\hat{Y}_P. \tag{13}$$

If we substitute these rescalings into Equations (3)–(8) then in region Ω_1

$$\frac{\partial \hat{Y}}{\partial \tau} = \bar{D}_Y \nabla^2 \hat{Y} + \bar{k}_6 \hat{Y}_P, \tag{14}$$

$$\frac{\partial \hat{Y}_P}{\partial \tau} = \nabla^2 \hat{Y}_P - \bar{k}_6 \hat{Y}_P, \tag{15}$$

and in regions Ω_2 and Ω_3

$$\frac{\partial \hat{A}}{\partial \tau} = -\hat{A} + \bar{k}_2 \hat{A}_P \hat{Y}, \tag{16}$$

$$\frac{\partial \hat{A}_P}{\partial \tau} = \hat{A} - \bar{k}_2 \hat{A}_P \hat{Y}, \tag{17}$$

$$\frac{\partial \hat{Y}}{\partial \tau} = \bar{D}_Y \nabla^2 \hat{Y} - \alpha \bar{k}_2 \hat{A}_P \hat{Y} + (\bar{k}_4 + \bar{k}_6)\hat{Y}_P, \tag{18}$$

$$\frac{\partial Y_P}{\partial \tau} = \nabla^2 \hat{Y}_P + \alpha \bar{k}_2 \hat{A}_P \hat{Y} - (\bar{k}_4 + \bar{k}_6)\hat{Y}_P, \tag{19}$$

where:

$$\bar{k}_2 = \frac{k_2 Y_T}{k_1},\ \bar{k}_4 = \frac{k_4 Z}{k_1},\ \bar{k}_6 = \frac{k_6}{k_1},\ \alpha = \frac{A_T}{Y_T} \text{ and } \bar{D}_Y = \frac{D_Y}{D_{YP}}, \tag{20}$$

are defined as the non-dimensional parameters. The number of parameters has been reduced from nine (k_1, k_2, k_4, k_6, D_Y, D_{YP}, A_T, Y_T, Z) to five ($\bar{k}_2, \bar{k}_4, \bar{k}_6, \bar{D}_Y, \alpha$).

The initial and boundary conditions are also rescaled such that in Ω_1,

$$\hat{Y}(\hat{\mathbf{x}},0) = 1 \qquad \text{and} \qquad \hat{Y}_P(\hat{\mathbf{x}},0) = 0 \tag{21}$$

and in Ω_2 and Ω_3

$$\hat{A}(\hat{\mathbf{x}},0) = 1,\ \hat{A}_P(\hat{\mathbf{x}},0) = 0,\ \hat{Y}(\hat{\mathbf{x}},0) = 1 \text{ and } \hat{Y}_P(\hat{\mathbf{x}},0) = 0 \tag{22}$$

with the boundary conditions now given by:

$$\hat{\mathbf{n}} \cdot \nabla \hat{Y}(\hat{\mathbf{x}}, t) = 0 \qquad \text{and} \qquad \hat{\mathbf{n}} \cdot \nabla \hat{Y}_P(\hat{\mathbf{x}}, t) = 0. \tag{23}$$

Here we have assumed that initially all of the CheY and CheA is unphosphorylated such that $Y_0 = Y_T$ and $A_0 = A_T$.

4.2 Parameterizing the model

To date we have formulated a spatio-temporal mathematical model of intracellular signalling in a bacterial cell based upon certain assumptions. Each term in the equations represents a certain process, for instance the reaction or diffusion of certain proteins. The parameters associated with each of these terms tell us (given their magnitude) the relative importance of each process. In the case of our *E. coli* cell parameterizing the system is relatively straightforward, the respective dimensional and corresponding non-dimensional parameters are listed in *Table 2*.

The non-dimensional parameters show that in terms of importance phosphotransfer from $CheA_P$ to CheY is the dominant reaction process ($\bar{k}_2 = 28.53$), autophosporylation of CheA (our non-dimensionalization means this process is of order one), followed by dephosphorylation of $CheY_P$ by CheZ ($\bar{k}_4 = 0.179$) and finally the natural dephosphorylation of $CheY_P$ ($\bar{k}_6 = 2.5 \times 10^{-3}$).

4.3 *Model solutions and results*

We solve Equations (14)–(19), with their respective boundary and initial conditions, using the computational package COMSOL (Stockholm, Sweden). COMSOL uses the theory of finite elements to solve PDEs and allows dynamical behaviour to be studied in detail. *Figures 3A–D* (see colour plate section) show the change in concentration of $CheY_P$ at various time steps of the simulation. We note these results show the diffusion of $CheY_P$ from the receptor poles, where it is created, towards the centre of the cell. The $CheY_P$ diffuses through the cell at a rate dependent upon the magnitude of its diffusion coefficient.

$$\bar{k}_2 = \frac{k_2 Y_T}{k_1},\ \bar{k}_4 = \frac{k_4 Z}{k_1},\ \bar{k}_6 = \frac{k_6}{k_1},\ \alpha = \frac{A_T}{Y_T} \text{ and } \bar{D}_Y = \frac{D_Y}{D_{YP}}, \tag{20}$$

are defined as the non-dimensional parameters. The number of parameters has been reduced from nine (k_1, k_2, k_4, k_6, D_Y, D_{YP}, A_T, Y_T, Z) to five ($\bar{k}_2, \bar{k}_4, \bar{k}_6, \bar{D}_Y, \alpha$).

The initial and boundary conditions are also rescaled such that in Ω_1,

$$\hat{Y}(\hat{\mathbf{x}},0) = 1 \qquad \text{and} \qquad \hat{Y}_P(\hat{\mathbf{x}},0) = 0 \tag{21}$$

and in Ω_2 and Ω_3

$$\hat{A}(\hat{\mathbf{x}},0) = 1,\ \hat{A}_P(\hat{\mathbf{x}},0) = 0,\ \hat{Y}(\hat{\mathbf{x}},0) = 1 \text{ and } \hat{Y}_P(\hat{\mathbf{x}},0) = 0 \tag{22}$$

with the boundary conditions now given by:

$$\hat{\mathbf{n}} \cdot \nabla \hat{Y}(\hat{\mathbf{x}}, t) = 0 \qquad \text{and} \qquad \hat{\mathbf{n}} \cdot \nabla \hat{Y}_P(\hat{\mathbf{x}}, t) = 0. \tag{23}$$

Here we have assumed that initially all of the CheY and CheA is unphosphorylated such that $Y_0 = Y_T$ and $A_0 = A_T$.

4.2 Parameterizing the model

To date we have formulated a spatio-temporal mathematical model of intracellular signalling in a bacterial cell based upon certain assumptions. Each term in the equations represents a certain process, for instance the reaction or diffusion of certain proteins. The parameters associated with each of these terms tell us (given their magnitude) the relative importance of each process. In the case of our *E. coli* cell parameterizing the system is relatively straightforward, the respective dimensional and corresponding non-dimensional parameters are listed in *Table 2*.

The non-dimensional parameters show that in terms of importance phosphotransfer from $CheA_P$ to CheY is the dominant reaction process ($\bar{k}_2 = 28.53$), autophosporylation of CheA (our non-dimensionalization means this process is of order one), followed by dephosphorylation of $CheY_P$ by CheZ ($\bar{k}_4 = 0.179$) and finally the natural dephosphorylation of $CheY_P$ ($\bar{k}_6 = 2.5 \times 10^{-3}$).

4.3 *Model solutions and results*

We solve Equations (14)–(19), with their respective boundary and initial conditions, using the computational package COMSOL (Stockholm, Sweden). COMSOL uses the theory of finite elements to solve PDEs and allows dynamical behaviour to be studied in detail. *Figures 3A–D* (see colour plate section) show the change in concentration of $CheY_P$ at various time steps of the simulation. We note these results show the diffusion of $CheY_P$ from the receptor poles, where it is created, towards the centre of the cell. The $CheY_P$ diffuses through the cell at a rate dependent upon the magnitude of its diffusion coefficient.

5 Summary and future work

A spatio-temporal model of the phosphotransfer pathway within *E. coli* has been produced using the mathematical theory of reaction-diffusion equations. Solutions to the model have allowed us to examine the way in which the concentration of $CheY_P$ dynamically changes within the cell. The model results show the creation of $CheY_P$ at the receptor clusters which then diffuses towards the centre of the cell.

The modelling approach here differs from that of Lipkow *et al.* (2005), who undertook stochastic simulations involving each model protein. Lipkow *et al.* (2005) also considered the interaction between $CheY_P$ and the motor protein FliM, which we have not included here. However, although our approach has differed we have been able to reproduce the same findings in respect of the location of CheZ (results not shown). The model developed here will be extended further in future research to incorporate the CheB pathway. We will also use this approach to understand the importance of spatial protein localization in the more complex signal transduction system of *Rhodobacter sphaeroides* (Porter and Armitage, 2002).

This work demonstrates that although there are different approaches to modelling a biological problem, each theoretical technique can tell us something about the system that another may not be able to and *vice versa*. This demonstrates the strengths of theoretical models in being able to provide various insights into the biological system being analysed.

Although modelling approaches have been used to understand certain parts of the bacterial chemotaxis system, there still remain a number of unanswered questions, both on the individual and population scale. Of growing interest is how individual cell behaviour affects the overall growth and development of a population. Such work requires the use of multi-scale modelling (Tindall *et al.*, in press) which allows individual behaviour to be incorporated into population models. For instance, recent work by Bray *et al.* (2007) has demonstrated the importance of adaptation on the accumulation of bacteria in response to attractant gradients.

The application of mathematical models to problems in the biological sciences can provide valuable insight into the system being studied. It is important that models are based upon known biological evidence and are developed in strong collaborations between theoreticians and experimentalists. This approach leads to models being used to test certain hypotheses, helps direct future experimental work and thereby provide insight to the biological problem at hand. In short these points are the real strengths of systems biology.

Acknowledgements

This work (MJT) was funded by a grant (BB/C513350/1) from the Biotechnology and Biological Sciences Research Council (BBSRC), UK. PKM was partly supported by a Royal Society Merit Award.

References

Adler, J. (1966) Chemotaxis in bacteria. *Science* **153:** 708–716.

Barkai, N. & Leibler, S. (1997) Robustness in simple biochemical networks. *Nature* **387:** 913–917.

Block, S., Segall, J. & Berg, H. (1982) Impulse response in bacterial chemotaxis. *Cell* **31:** 215–226.

Block, S., Segall, J. & Berg, H. (1983) Adaptation kinetics in bacterial chemotaxis. *J. Bacteriol.* **154:** 312–323.

Bray, D., Bourret, R. & Simon, M. (1993) Computer simulation of the phosphorylation cascade controlling bacterial chemotaxis. *Mol. Biol. Cell* **4:** 469–482.

Bray, D., Levin, M. & Morton-Firth, C. (1998) Receptor clustering as a cellular mechanism to control sensitivity. *Nature* **393(7):** 85–88.

Bray, D., Levin, M. & Lipkow, K. (2007) The chemotactic behavior of computer-based surrogate bacteria. *Curr. Biol.* **17:** 12–19.

Cantwell, B., Draheim, R., Weart, R., Nguyen, C., Stewart, R. & Manson, M. (2003) CheZ phosphatase localizes to chemoreceptor patches via CheA-short. *J. Bacteriol.* **185(7):** 2354–2361.

Eisenbach, M., Lengeler, J., Varon, M. *et al.* (2004) *Chemotaxis.* Imperial College Press, London.

Elowitz, M., Surette, M., Wolf, P., Stock, J. & Leibler, S. (1999) Protein mobility in the cytoplasm of *Escherichia coli. J. Bacteriol.* **181(1):** 197–203.

Emonet, T., Macal, C., North, M., Wickersham, C. & Cluzel, P. (2005) Agentcell: a digital single-cell assay for bacterial chemotaxis. *Bioinformatics* **21(11):** 2714–2721.

Erban, R. & Othmer, H. (2004) From individual to collective behaviour in bacterial chemotaxis. *SIAM J. Appl. Math.* **65:** 361–391.

Francis, N., Levit, M., Shaikh, T., Melanson, L. & Stock, J. (2002) Subunit organization in a soluble complex of Tar, CheW and CheA by electron microscopy. *J. Biol. Chem.* **277:** 36755–36759.

Goldbeter, A. & Koshland, D. (1982) Simple molecular model for sensing and adaptation based on receptor modification with application to bacterial chemotaxis. *J. Mol. Biol.* **161:** 395–416.

Keller, E. & Segel, L. (1971) Travelling bands of chemotactic bacteria: A theoretical analysis. *J. Theor. Biol.* **30(2):** 235–248.

Kreft, J., Booth, G. & Wimpenny, J. (1998) Bacsim, a simulator for individual-based modelling of bacterial colony growth. *Microbiology* **144:** 3275–3287.

Li, M. & Hazelbauer, G. (2004) Cellular stoichiometry of the components of the chemotaxis signalling complex. *J. Bacteriol.* **186:** 3687–3694.

Liberman, L., Berg, H. & Sourjik, V. (2004) Effect of chemoreceptor modification on assembly and activity of the receptor-kinase complex in *Escherichia coli. J. Bacteriol.* **186:** 6643–6646.

Lipkow, K. (2006) Changing cellular location of CheZ predicted by molecular simulations. *PLoS Comput. Biol.* **2(4):** 301–310.

Lipkow, K., Andrews, S. & Bray, D. (2005) Simulated diffusion of phosphorylated CheY through the cytoplasm of *Escherichia coli. J. Bacteriol.* **187(1):** 45–53.

Murray, J. (1993) *Mathematical Biology*, 2nd Edn. Springer Verlag, Berlin.

Porter, S. & Armitage, J. (2002) Phosphotransfer in *Rhodobacter sphaeroides* chemotaxis. *J. Mol. Biol.* **324:** 35–45.

Porter, S., Wadhams, G., Martin, A., Byles, E., Lancaster, D. & Armitage, J. (2006) The CheYs of *Rhodobacter sphaeroides. J. Biol. Chem.* **281(43):** 32694–32704.

Rao, C., Kirby, J. & Arkin, A. (2004) Design and diversity in bacterial chemotaxis: a comparative study in *Escherichia coli* and *Bacillus subtilis. PLoS Biol.* **2(2):** 239–252.

Segall, J., Ishihara, A. & Berg, H. (1985) Chemotactic signalling in filamentous cells of *Escherichia coli*. *J. Bacteriol.* **161(1):** 51–59.

Segall, J., Block, S. & Berg, H. (1986) Temporal comparisons in bacterial chemotaxis. *Proc. Natl Acad. Sci.* USA **83(23):** 8987–8991.

Segel, L. & Goldbeter, A. (1986) A mechanism for exact sensory adaptation based on receptor modification. *J. Theor. Biol.* **120:** 151–179.

Shrout, A., Montefusco, D. & Weis, R. (2003) Template-directed assembly of receptor signalling complexes. *Biochemistry-US* **42(46):** 13379–13385.

Smith, J., Latiolais, J., Guanga, G., Citineni, S., Silversmith, R. & Bourret, R. (2003) Investigation of the role of electrostatic charge in activation of the *Escherichia coli* response regulator CheY. *J. Bacteriol.* **185(21):** 6385–6391.

Sourjik, V. & Berg, H. (2002a) Binding of the *Escherichia coli* response regulator CheY to its target measured in vivo by fluorescence resonance energy transfer. *Proc. Natl Acad. Sci.* USA **99:** 12669–12674.

Sourjik, V. & Berg, H. (2002b) Receptor sensitivity in bacterial chemotaxis. *Proc. Natl Acad. Sci.* USA **99(1):** 123–127.

Spiro, P., Parkinson, J. & Othmer, H. (1997) A model of excitation and adaptation in bacterial chemotaxis. *Proc. Natl Acad. Sci.* USA **94:** 7263–7268.

Stewart, R. & van Bruggen, R. (2004) Rapid phosphotransfer to CheY from a CheA protein lacking the CheY-binding domain. *Biochemistry-US* **43(27):** 8766–8777.

Stewart, R., Jahreis, K. & Parkinson, J. (2000) Rapid phosphotransfer to CheY from a CheA protein lacking the CheY-binding domain. *Biochemistry-US* **39(43):** 13157–13165.

Tindall, M., Maini, P., Porter, S. & Armitage, J. (2007a) Overview of mathematical approaches used to model bacterial chemotaxis II: Bacterial populations. *Bull. Math. Biol.*, In press.

Tindall, M., Porter, S., Maini, P., Gaglia, G. & Armitage, J. (2007b) Overview of mathematical approaches used to model bacterial chemotaxis I: The single cell. *Bull. Math. Biol.*, In press.

Wadhams, G. & Armitage, J. (2004) Making sense of it all: Bacterial chemotaxis. *Nat. Rev. Mol. Cell Biol.* **5(12):** 1024–1037.

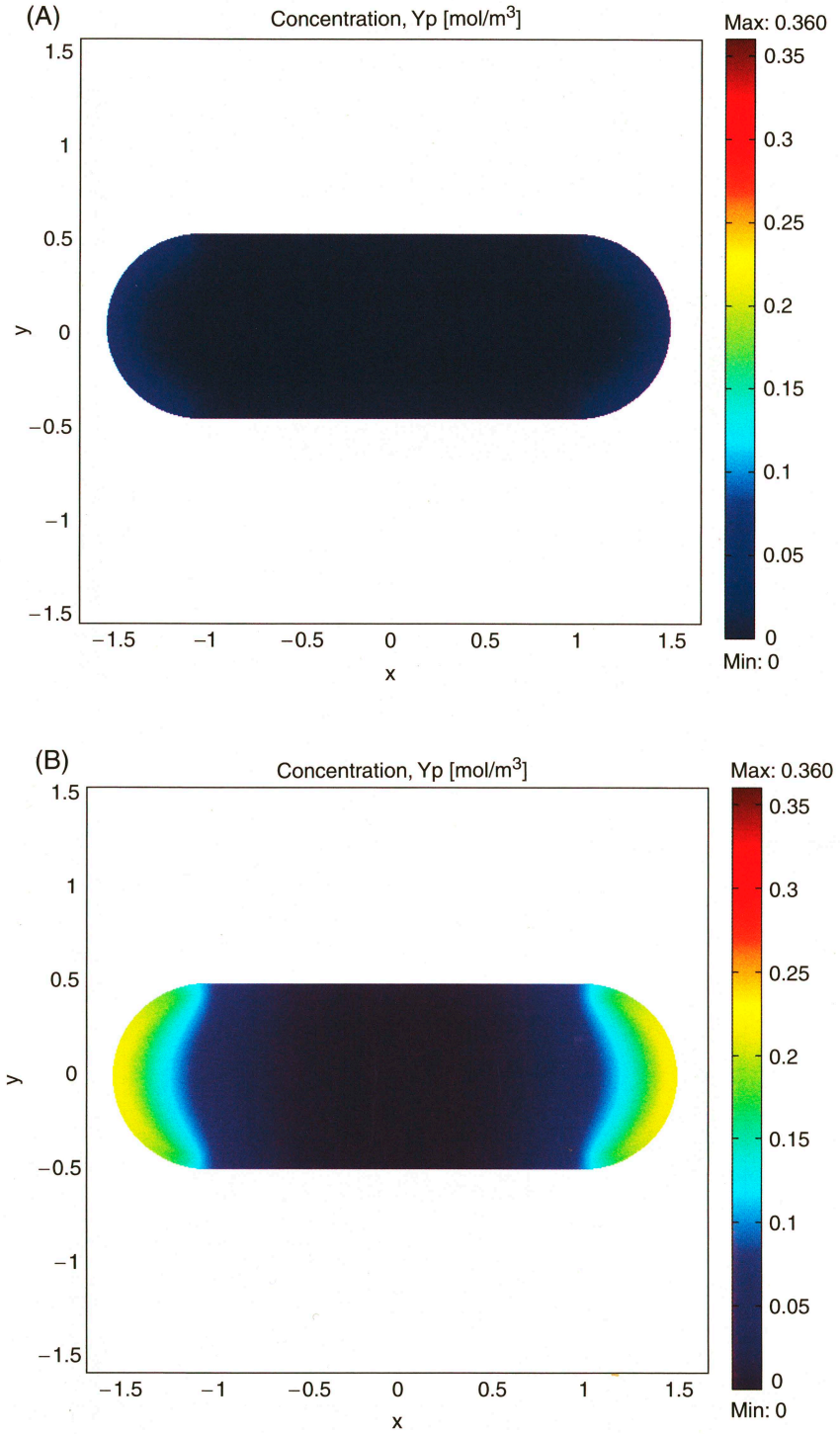

Chapter 8, Figure 3. The dynamic change in the non-dimensional concentration of $CheY_P$ within an E. coli cell at (*A*) 2 ms, (*B*) 10 ms, (*C*) 20 ms, and (*D*) 40 ms. Here the cell has been taken to be 3 μm long and 1 μm wide.

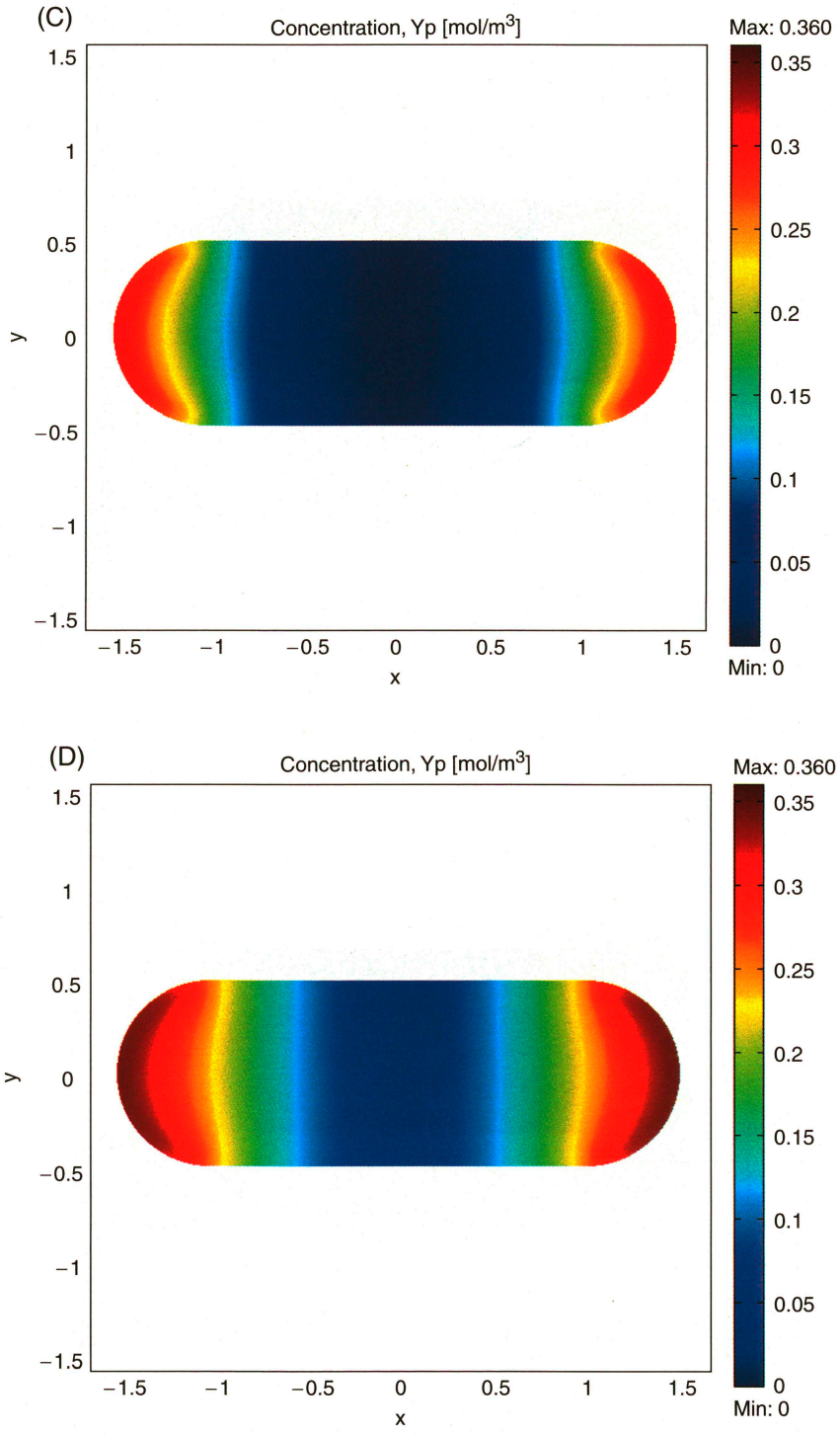

Chapter 8, Figure 3. cont'd.